

Dissipative standard map

G. Schmidt and B. W. Wang*

Department of Physics, Stevens Institute of Technology, Hoboken, New Jersey 07030

(Received 22 May 1985)

The transition from Hamiltonian to dissipative systems is studied. In the dissipative standard map the area-preserving map becomes dissipative as the dissipation parameter is varied and ultimately turns into a one-dimensional circle map. All periodic orbits on the Hamiltonian map go over smoothly into orbits in the circle map. Many-piece strange attractors on the one-dimensional map are gradually wiped out as the dissipation disappears.

INTRODUCTION

The standard map is one of the most widely studied area-preserving (Hamiltonian) maps.¹⁻⁹ Like all maps corresponding to nonintegrable Hamiltonian systems, it has stable and unstable periodic orbits, Kolmogorov-Arnol'd-Moser (KAM) surfaces, and chaotic regions. As the nonintegrability parameter is increased KAM surfaces disintegrate, and chaotic regions spread. It has a "last" KAM surface at the golden-mean rotation number² a member of the most robust, noble KAM surfaces⁷ whose rotation numbers have continued-fraction expansion ending in an infinite sequence of 1's [$a, b, c, \dots, 1, 1, 1, \dots$]. The stability properties of any KAM surface can be inferred from the stability of periodic orbits with rotation numbers convergent to that of the KAM surface. A convenient way of viewing the stability properties of these surfaces is by constructing fractal diagrams.⁴ When stable periodic orbits become unstable they appear to go through universal period-doubling sequences.¹⁰

Here we study the dissipative standard map¹¹

$$\begin{aligned}x' &= x + y', \\ y' &= by + (K/2\pi)\sin(2\pi x).\end{aligned}\quad (1)$$

When $b=1$ this is just the standard map with the nonlinearity parameter K . When the "dissipation parameter" b (the Jacobian of the map) equals unity, the two-dimensional map has contracted to a line and the one-dimensional circle map

$$x' = x + (K/2\pi)\sin(2\pi x) = f(x) \quad (2)$$

results. We study the range $0 \leq b \leq 1$. Equation (1) can be written as a difference equation

$$\begin{aligned}x_{n+1} - 2x_n + x_{n-1} + (1-b)(x_n - x_{n-1}) \\ = (K/2\pi)\sin(2\pi x_n).\end{aligned}$$

The corresponding differential equation obviously describes the damped pendulum with the damping rate $1-b$.

While the standard map has symmetries in x and y so

that the map of the plane reduces to the map of the torus $0 \leq x \leq 1$, $0 \leq y \leq 1$, the symmetry in y is broken when $b \neq 1$ and our map is a map of the cylinder $0 \leq x \leq 1$, $-\infty \leq y \leq \infty$.

When studying the stability domains of periodic orbits in the K - b parameter plane (an extension of the fractal diagram⁴), it appears that all stable periodic orbits on the Hamiltonian map connect continuously all the way to the one-dimensional map. This is remarkable since the Hamiltonian map has an infinity of stable periodic orbits for a fixed K , while the circle map has essentially only one stable orbit for a given value of K . The periodic orbits map from the three-dimensional K - x - y space (for $b=1$) to the two-dimensional K - x plane for $b=0$.

Recently Holmes studied¹² the quadratic Hénon map with a dissipation parameter connecting the one-dimensional quadratic map with the area-preserving quadratic map. He found that the stable orbits of the one-dimensional map connect with the area-preserving limit. It is perhaps even more remarkable that the inverse appears also to be true for a map as rich as the standard map.

In fact we find that there are orbits of the one-dimensional map that have no counterpart in the Hamiltonian map. For the circle map (2), just like for the 1D quadratic map,¹³ the period-doubling sequence ends at some K_∞ . When $K > K_\infty$ an inverse bifurcation sequence of bands results, giving rise to 2^n -piece strange attractors. With increasing K this sequence merges until only a one-piece strange attractor is left. We find that as b is increased this sequence is gradually wiped out so in the Hamiltonian limit when $K > K_\infty$ only connected (one piece) chaos is found. This is intuitively satisfying since Hamiltonian multipiece chaos could only exist if local KAM surfaces survived for $K > K_\infty$.

The attractive bands (strange attractors) of the 1D map undergo an infinite sequence of crises,¹⁴ where a small change in K results in transitions from strange to regular attractors and back again. This may be called "sensitive dependence on the parameter." We find that this behavior persists for finite b values. This lack of structural stability is of concern for experimental observations, since a slight variation of parameter values during the course of the experiment is unavoidable.

PERIODIC ORBITS

There are two types of periodic orbits for area-preserving maps. One type is unstable for any value of the parameter, the other is stable for a range in K , and typically becomes unstable via a period-doubling bifurcation sequence, at some parameter value K_c . For the standard map, periodic orbits are conveniently characterized by their rotation number.² If an orbit has period Q , and the number of rotations executed in Q iterations either on the torus or around a fixed point is R , the rotation number is $r = R/Q$. The fractal diagram is formed by plotting the K_c values for rational rotation numbers by family. The points for each family exhibit an ordered pattern.⁴

We wish now to calculate the extension of the fractal diagram to the dissipative case.

The period-one orbit with rotation number $0/1$ is calculated from

$$\begin{aligned} x' &= x = x + by + (K/2\pi)\sin(2\pi x), \\ y' &= y = by + (K/2\pi)\sin(2\pi x), \end{aligned} \quad (3)$$

with solution $x = \frac{1}{2}$, $y = 0$ ($x = 0$, $y = 0$ is always unstable). Stability can be determined from the eigenvalue equation of the Jacobian matrix

$$\lambda^2 - (\text{Tr}J)\lambda + b = 0, \quad (4)$$

where the trace of the Jacobian matrix, $\text{Tr}J = 1 - K + b$. The orbit is stable when $|\lambda| \leq 1$, $0 < K < 2(1+b)$. At the upper limit $K_c = 2(1+b)$, $\lambda = -1$, so there is a period-doubling bifurcation at this point.

The period-two orbit created by this bifurcation consists of a pair of points with $x' = 1 - x$, $y' = -y$ ($x'' = x$, $y'' = y$). From Eq. (1)

$$1 - 2x = [K/2\pi(1+b)]\sin(2\pi x). \quad (5)$$

For the once iterated Jacobian

$$\text{Tr}J = 1 + K^2 \cos^2(2\pi x) + 2K(1+b)\cos(2\pi x) + b^2,$$

and the eigenvalue equation is $\lambda^2 - (\text{Tr}J)\lambda + b^2 = 0$. The range of stability is $2(1+b) < K < \pi(1+b)$. The lower limit is the K value where this orbit is born by bifurcation of the period-one orbit, while at the upper limit the orbit becomes unstable. Since $\lambda = +1$ at the upper limit it does not give rise to a period-four orbit but two period-two orbits.

For these orbits $x' = x + \frac{1}{2}$, $y' = -y$ which yields for the location of the four x values $K\sin(2\pi x) = \pm\pi(1+b)$. The stability calculation can again be carried out without difficulty to find

$$\pi(1+b) < K < [2(1+b^2) + \pi^2(1+b)^2]^{1/2}.$$

At the upper limit $\lambda = -1$, and both period-two orbits bifurcate into period-four orbits. Further bifurcation can be obtained numerically. They are period doubling with $Q = 2^n$, and $n \rightarrow \infty$ at the K_∞ line shown in Fig. 1.

The period-one family contains orbits with arbitrary integer rotation numbers. These orbits are located at

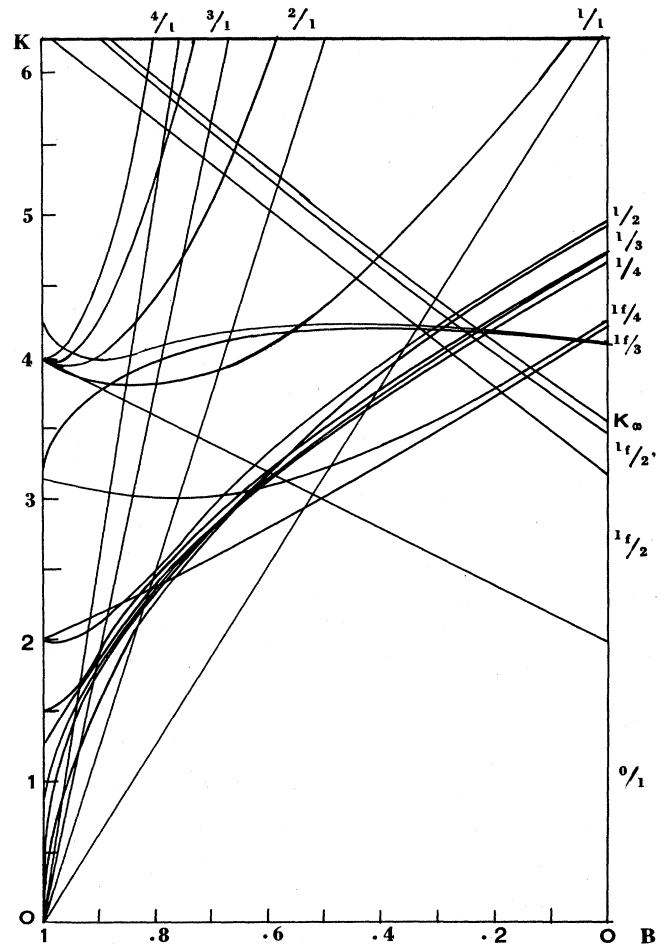


FIG. 1. Parameter-space diagram of stable periodic orbits, for different rotation numbers. Index f signifies orbits rotating around the fixed point $0.5, 0$ rather than around the cylinder. Period 2 bifurcates into $2'$.

$$\begin{aligned} x' &= x + R = x + by + (K/2\pi)\sin(2\pi x), \\ y' &= y = by + (K/2\pi)\sin(2\pi x). \end{aligned} \quad (6)$$

Expressing y from the second equation and substituting into the first one results in

$$R = [K/2\pi(1-b)]\sin(2\pi x)$$

and $y = R$. The stability calculation leads for these $r = R/1$ orbits,

$$2\pi R(1-b) < K_R < 2[\pi^2(1-b)^2 R^2 + (1+b)^2]^{1/2}.$$

These orbits are born at the lower limit as tangent bifurcations and become unstable at the upper limit via period-doubling bifurcations. The range of stable existence of some of these orbits in the K - b parameter space is also shown on Fig. 1.

There is another set of period-two orbits where the stability limits can be analytically calculated. These are the $x'' = x$ orbits (note that $x'' = x + \text{integer}$ are also period-

two not calculated here). These all have solutions $y' = -y$ and $\sin 2\pi x + \sin 2\pi x' = 0$. For details see Appendix A. Two types of solutions exist: $x' = m - x$ and $x' = x + m - \frac{1}{2}$ with m integer.

The first type, $x' = m - x$, is born at $K_m = (1+b)q_m$, where the q_m values are calculated in Appendix A. The orbit is stable in the range

$$(1+b)q_m < K < 2\pi(1+b)(m - \frac{1}{2}).$$

When the upper limit is reached these orbits become unstable and give rise to period-two orbits of the second type, $x' = x + m - \frac{1}{2}$, with a range of stability

$$2\pi(1+b)(m - \frac{1}{2}) < K < [2(1+b^2) + (2\pi)^2(m - \frac{1}{2})^2(1+b)^2]^{1/2}.$$

At the upper limit $\lambda = -1$ so the orbits destabilize via period-doubling bifurcations.

The stability limits of several other orbits have been extended numerically from the Hamiltonian ($b = 1$) case to the one-dimensional limit. Some of these orbits have been plotted in the parameter-space diagram in Fig. 1. We find that all orbits calculated with a range of stability in the Hamiltonian map extend all the way to the one-dimensional map. As the Hamiltonian map accommodates an infinity of stable orbits for a given value of the parameter K , the stability regions become narrower in parameter space, and separate, as b is reduced. For a given b as K is increased the orbits are born by a tangent bifurcation and destabilize by period doubling. When $b = 0$ there are at most a finite number of stable orbits for a given value of K .

Orbits of the one-dimensional circle map have been

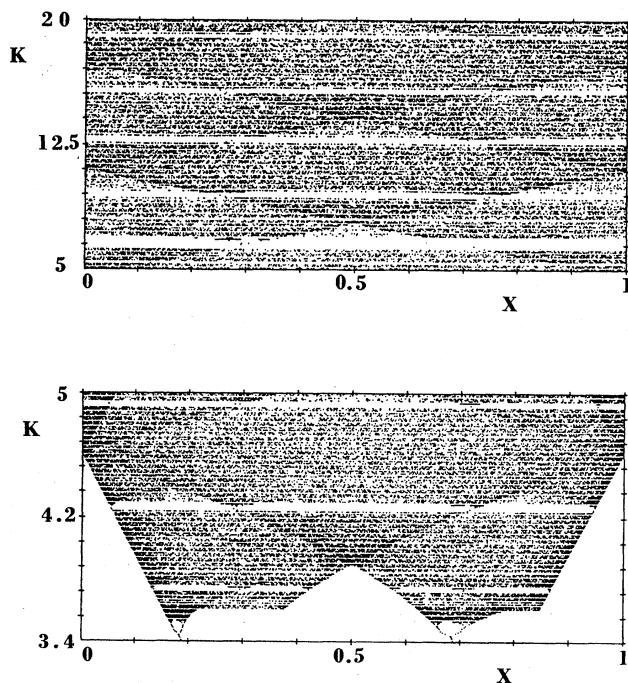


FIG. 2. Attractors of the circle map $x' = x + (K/2\pi)\sin(2\pi x)$.

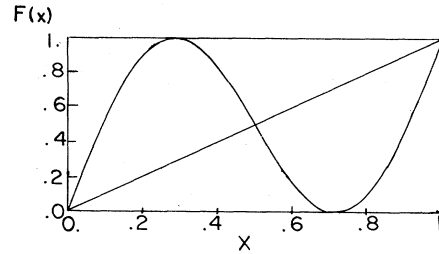


FIG. 3. Construction for the calculation of K_L , the smallest K to give orbits rotating on the cylinder.

plotted in Fig. 2. As K is increased starting from $K = 0$ a period-doubling bifurcation sequence, similar to that of the quadratic map, takes place. When $K_\infty = 3.5315$ is surpassed, bands (strange attractors) of period 2^n are formed and merge finally into a single band. The bands are interrupted by the sudden appearance of stable periodic orbits of finite period followed by their own bifurcation sequences. While this fact is a well-known characteristic of one-dimensional maps it appears now in a new light; the periodic orbits are the extensions of the Hamiltonian orbits that have no other place to go.

Unlike the quadratic map, the circle map extends all the way to $K \rightarrow \infty$, and so do the interruptions by stable periodic orbits. The most important of these (producing the largest gaps in Fig. 2), correspond to the period-one and period-two stable orbits calculated above.

The orbits that rotate on the cylinder for $b \neq 0$ make their appearance on the circle map when a critical parameter value $K_L = 4.60333$ has been surpassed. The construction of Fig. 3 shows how this value is calculated. The condition that successive mappings of a point in the $0 < x < 1$ interval can ultimately carry it outside this region is that the first maximum of $f(x) = f_m(x) > 1$. This condition leads to the equations for the threshold

$$\begin{aligned} K_L \sin \xi &= 2\pi - \xi, \\ K_L \cos \xi &= -1, \end{aligned} \tag{7}$$

where $\xi = 2\pi x_0$ and x_0 is the position of the maximum. These equations yield $\xi = 1.789776$ and $K_L = 4.60333$.

We have also calculated the ranges of stability of some golden-mean convergents. Details are given in Appendix B. On the circle map the K values of these converge very rapidly, and the range of K where they exist becomes very narrow as the Fibonacci numbers (whose ratio is the rotation number) are increased. In the Hamiltonian map these orbits converge to the golden-mean KAM surface. When $b < 1$ they converge to a stable orbit of infinite period which is no longer continuous and whose range of stability in K has shrunk to zero.

STRANGE ATTRACTORS

Chaos appears in the one-dimensional map as $K > K_\infty$ as a set of bands of period 2^n , where $n \rightarrow \infty$ as $K \rightarrow K_\infty$ and the period becomes one ($n = 0$) at some finite value of K . When $1 > b > 0$ one expects these bands to become

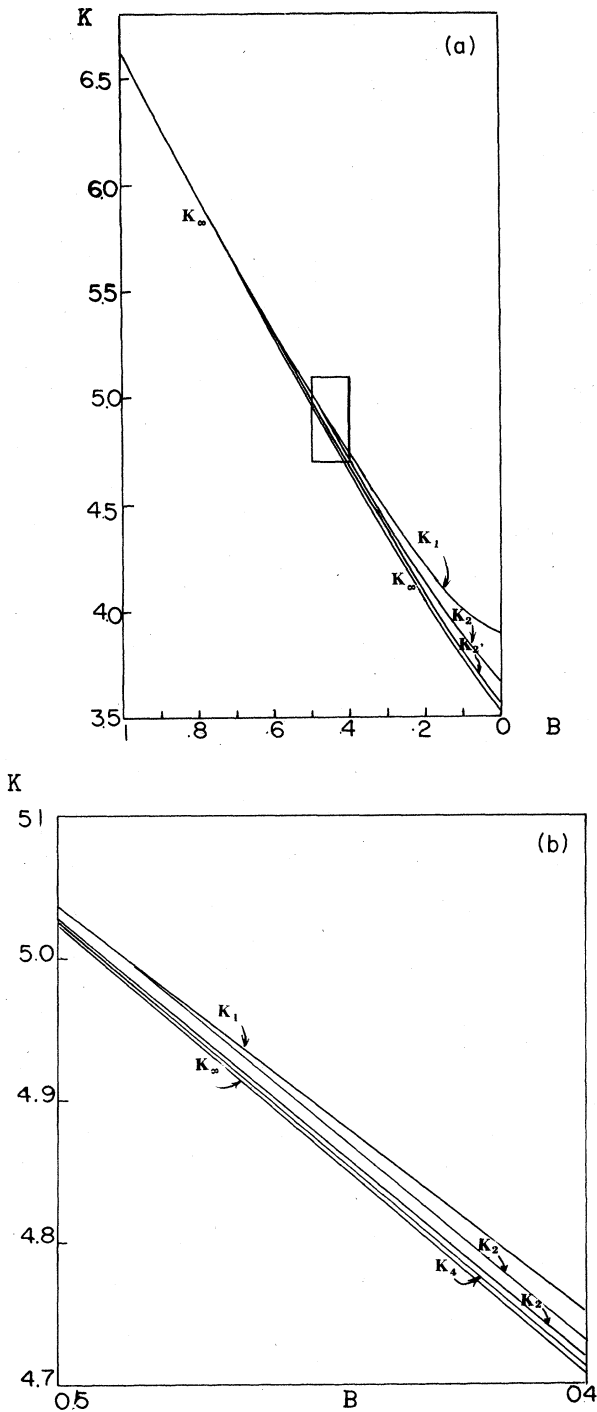


FIG. 4. Parameter-space diagram for multiple-piece strange attractors. (a) shows $0 < B < 1$, (b) is a magnification of region shown in (a).

2^n -piece strange attractors. As $b \rightarrow 1$ the strange attractor should correspond to a chaotic region bounded by KAM surfaces. However as $K \rightarrow K_\infty$ for a Hamiltonian orbit all KAM surfaces in the neighborhood are destroyed excluding the possibility of the emergence of 2^n -piece chaos.

We computed the boundaries in parameter space where

the strange attractors, arising from the bifurcations of the $x = \frac{1}{2}, y = 0$ fixed point, exist. This is shown in Fig. 4. The $K_\infty(b)$ is a smooth curve in the $0 < b < 1$ interval. The curve that represents the emergence of the one-piece strange attractor $K_1(b)$ connects with $K_\infty(1)$. The region $K_\infty < K < K_1$ shrinks to a point on the Hamiltonian side of the diagram. The curves $K_n(b)$ representing the lower boundary of 2^n -piece chaos terminate in K_1 .

To show this better we have plotted the $\ln(K_n - K_\infty)$ versus b curves shown in Fig. 5. (There are two different $n = 2$ lines for our map, designated by 2 and 2', arising from a symmetry, just as the period-two stable orbit bifurcates into a pair of period-two orbits.) For a given $b \neq 1$ typically one finds that the inverse bifurcation sequence of many-piece strange attractors terminates at some finite n and becomes a one-piece attractor.

We have studied the destruction mechanism of the many-piece strange attractors as the dissipation is reduced. When $b = 0$ there is just one (or in case of degeneracy a finite number) chaotic orbit at a given value of the parameter K . When b is increased more and more stable as well as unstable trajectories coexist in the x - y plane. Thus for a given K and $b \neq 1$ there are many unstable periodic orbits of different periods in the x - y plane, each with its stable and unstable invariant manifolds. The unstable invariant manifolds are potential strange attractors. The heteroclinic intersections of the stable manifold of the period-one orbit with a 2^n -piece strange attractor create a crisis leading to the destruction of the attractor.

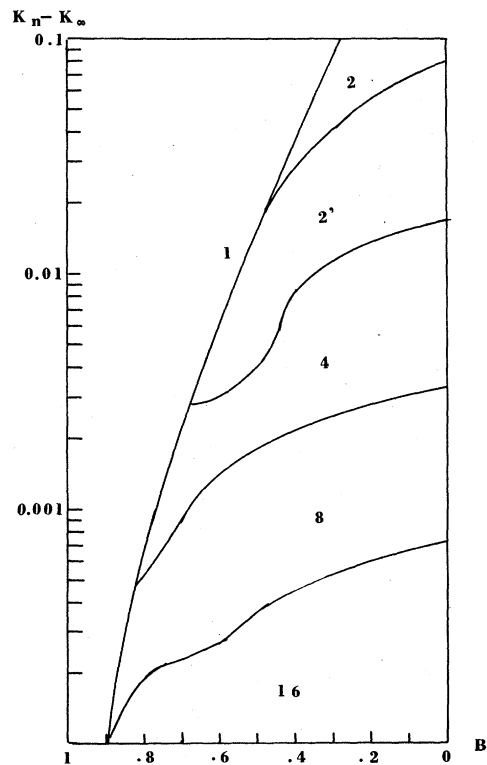


FIG. 5. $\ln(K_n - K_\infty)$ is plotted versus B for multiple-piece strange attractors.

Finally, a remark shall be made about a phenomenon that may be termed "sensitive dependence on the parameter." In the one-dimensional map above K_∞ the bands are interrupted by periodic orbits. These orbits are dense in K so that arbitrarily close to a K value exhibiting chaos there are many parameter values where periodic orbits rather than chaos exists. If one carried out an experiment, where the behavior of a physical quantity was described by the map, a slight drift in the physical parameter corresponding to K would carry the system to a region characterized by qualitatively different behavior. This lack of structural stability would render the interpretation of the experimental results virtually impossible.

The Hamiltonian map does not suffer from this difficulty. As K is varied the behavior of the map varies smoothly, except for isolated K values like the one where the golden-mean KAM surface breaks. As we have seen, as b is reduced, the objects that appeared separated in x - y , become increasingly separated in parameter space giving rise to the sensitive dependence on the parameter. It appears from numerical evidence that the change is gradual. As b is increased the interruptions of the chaotic bands by stable periodic orbits gradually disappear. The periodic orbits causing the interruptions have moved to different positions in x - y space. One expects therefore that experiments on near-Hamiltonian systems with small dissipation will be more amenable to theoretical interpretation than nonintegrable strongly dissipative systems.

ACKNOWLEDGMENTS

The authors acknowledge illuminating conversations with M. J. Feigenbaum, R. Helleman, and E. Ott. This work was partially supported by U.S. Department of Energy Contract No. DE-AC02-84ER13146.

APPENDIX A

Consider the class of period-two orbits where $x''=x$ and $y''=y$. From $x=x''=x'+y''=x'+y$ and $x'=x+y'$ it follows that $y'=-y$. From $-y=y'=by'+(K/2\pi)\sin(2\pi x)$, $y=-[K/2\pi(1+b)]\sin(2\pi x)$, so

$$x'=x+[K/2\pi(1+b)]\sin(2\pi x). \quad (\text{A1})$$

From

$$\begin{aligned} x &= x'' = x' + y'' = x' + by' + (K/2\pi)\sin(2\pi x') \\ &= x' + [Kb/2\pi(1+b)]\sin(2\pi x) \\ &\quad + (K/2\pi)\sin(2\pi x'), \end{aligned}$$

$$x' = x - [Kb/2\pi(1+b)]\sin(2\pi x) - (K/2\pi)\sin(2\pi x'). \quad (\text{A2})$$

Subtracting (A2) from (A1) gives

$$\sin(2\pi x) + \sin(2\pi x') = 0. \quad (\text{A3})$$

There are two types of solution: (1) $x' = m - x$, (2) $x' = x + m - \frac{1}{2}$, where m is an integer.

For type (1) from (A1)

$$m - 2x = [K/2\pi(1+b)]\sin(2\pi x). \quad (\text{A3}')$$

Since $\cos(2\pi x) = \cos(2\pi x')$, we have

$$\begin{aligned} \text{Tr}J &= 1 + b^2 + K^2 \cos^2(2\pi x) + 2K(1+b)\cos(2\pi x) \\ &= [K\cos(2\pi x) + 1 + b]^2 - 2b \end{aligned}$$

with the range of stability

$$-(1-b)^2 \leq [K\cos(2\pi x) + 1 + b]^2 \leq (1+b)^2. \quad (\text{A4})$$

The left inequality is always satisfied, while the one on the right is satisfied for $-\frac{1}{4} < x < \frac{1}{4}$. The upper limit is the relevant one and it gives from (A3') the critical $K = K_c$,

$$K_c = 2\pi(1+b)(m - \frac{1}{2}). \quad (\text{A5})$$

For type-(2) orbits $\cos(2\pi x') = \cos(2\pi x)$ and

$$m - \frac{1}{2} = x' - x = [K/2\pi(1+b)]\sin(2\pi x), \quad (\text{A6})$$

where (A1) has been used. When $x = \frac{1}{4}$, (A6) becomes identical with (A5). This mode comes into existence where the first mode becomes unstable. The trace of the Jacobian is

$$\text{Tr}J = 1 + b^2 - K^2 \cos^2(2\pi x) \quad (\text{A7})$$

giving the stability range

$$0 \leq K^2 \cos^2(2\pi x) \leq 2(1+b^2). \quad (\text{A8})$$

The left inequality is again automatically satisfied, while the right one gives $2(1+b^2) = K_c^2 - K_c^2 \sin^2(2\pi x)$. Using (A6) gives for the stability limit

$$K_c = [2(1+b^2) + (2\pi)^2(m - \frac{1}{2})^2(1+b^2)]^{1/2}. \quad (\text{A9})$$

The onset of mode 1 can be calculated using (A3'), and setting the derivatives of the left and right side equal, $-2 = [K/(1+b)]\cos(2\pi x)$. With $\xi = 2\pi x$ this gives the equations

$$\xi - m\pi = \tan\xi \quad (\text{A10})$$

and

$$K/(1+b) = -2/\cos\xi. \quad (\text{A11})$$

Solving (A10) numerically and using (A11) gives

$$q_2 = K_0/(1+b) = 9.20671 \text{ for } m = 2,$$

$$q_3 = K_0/(1+b) = 15.58 \text{ for } m = 3,$$

etc., where K_0 designates the onset of mode 1.

APPENDIX B

We have calculated golden-mean convergent orbits on the one-dimensional circle map. The K ranges over which these orbits are stable become small very fast:

$$r = \frac{1}{2}, \quad 4.9113 < K < 4.92425,$$

$$r = \frac{2}{3}, \quad 5.804346 < K < 5.804985,$$

$$r = \frac{3}{5}, \quad 5.78435458 < K < 5.7843558,$$

$$r = \frac{5}{8}, \quad 5.801324906 < K < 5.801324915,$$

$$r = \frac{8}{13}, \quad 5.8013128798095156 < K < 5.801312879809548,$$

$$r = \frac{13}{21}, \quad 5.80132457516983852 < K < 5.80132457516983863.$$

*Permanent address: Department of Modern Physics, China University of Science and Technology, Hefei, Anhui, China.

¹B. V. Chirikov, *Phys. Rep.* **52**, 263 (1979).

²J. M. Greene, *J. Math. Phys.* **20**, 1183 (1979).

³G. Schmidt, *Phys. Rev. A* **22**, 2849 (1980).

⁴G. Schmidt and J. Bialek, *Physica* **5D**, 397 (1982).

⁵R. S. MacKay, J. D. Meiss, and I. C. Percival, *Physica* **13D**, 55 (1984).

⁶T. Bountis and R. H. G. Helleman, *J. Math. Phys.* **22**, 1867 (1981).

⁷R. S. MacKay, Doctoral thesis, Princeton University, 1982.

⁸D. S. Broomhead and G. Rowlands, *J. Phys. A* **16**, 9 (1983).

⁹C. F. F. Karney, A. B. Rechester, and R. B. White, *Physica*

4D, 425 (1982).

¹⁰J. M. Greene, R. S. MacKay, F. Vivaldi, and M.J. Feigenbaum, *Physica* **3D**, 468 (1981).

¹¹This map is related to the one studied by G. M. Zaslavsky, *Phys. Lett.* **69A**, 145 (1978).

¹²P. Holmes, *Phys. Lett.* **104A**, 299 (1984); P. Holmes and D. Whitley, *Philos. Trans. R. Soc. London, Ser. A* **311**, 43 (1984); see also Hassan El Hamouli and C. Mira, *C. R. Acad. Sci.* **293**, 525 (1981).

¹³P. Collet and J. P. Eckman, *Iterated Maps on the Interval as Dynamical Systems* (Birkhäuser, Basel, 1980).

¹⁴C. Grebogi, E. Ott, and J. Yorke, *Phys. Rev. Lett.* **48**, 1507 (1982); *Physica* **7D**, 181 (1983).